Nuclear Instruments and Methods in Physics Research B xxx (2017) xxx–xxx

Contents lists available at ScienceDirect

Nuclear Instruments and Methods in Physics Research B

journal homepage: www.elsevier.com/locate/nimb

Elongation of metallic nanoparticles at the interface of silicon dioxide and silicon nitride

Pablo Mota-Santiago [a,*], Felipe Kremer [b], Allina Nadzri [a], Mark Cameron Ridgway [a], Patrick Kluth [a]

[a] Department of Electronic Materials Engineering, Research School of Physics and Engineering, Australian National University, Canberra ACT 2601, Australia
[b] Centre for Advanced Microscopy, Australian National University, 131 Garran Road, Acton 2601, Australia

ARTICLE INFO

Article history:
Received 9 December 2016
Received in revised form 16 February 2017
Accepted 12 March 2017
Available online xxxx

Keywords:
Ion-irradiation
Metallic nanoparticles
Elongation
Anisotropy
TEM

ABSTRACT

In the process of shape transformation of metal nanoparticles (MNPs) embedded in dielectrics resulting from swift heavy-ion irradiation, key parameters such as the energy deposition threshold, the necessity of a molten track and the NP size have been identified for amorphous silicon dioxide. The extension of such parameters to other dielectrics is yet unclear. We present experimental evidence of the shape transformation of nearly spherical NPs located at the interface of amorphous silicon nitride and silicon dioxide thin layers upon irradiation with 185 MeV Au ions at fluences of 0.3 and 1×10^{14} cm^{-2}. After irradiation the ~16–18 nm diameter Au and Ag NPs transformed into continuous nano-rods exhibiting a high aspect ratio with a clear preference of elongation into the silicon dioxide layer. The results are discussed in the context of Thermal Spike calculations, which indicate that the track formation timescales may have an important influence on the NP elongation process.

1. Introduction

Dielectric materials containing embedded metallic nanostructures with controlled anisotropy are of great interests due to their magnetic [1], and linear and nonlinear optical response arising from their plasmonics properties [2–6]. One method to fabricate such structures is by synthesis of nanoparticles in a dielectric thin film system followed by swift heavy-ion irradiation, which induces a shape transformation of the typically spherical nanoparticles to well-aligned nano-rods. This shape transformation process of MNPs has been studied predominantly with silicon dioxide as the host matrix [1,7–9]; yet little work has been done in other materials with the exception of sapphire [6]. As the plasmonic response of these systems depends on the dielectric function of the host matrix [10], it is highly desired to extend the approach developed for silicon dioxide to other dielectric hosts.

It has previously been established that the energy deposited by swift heavy-ions can lead to the formation of so called "ion tracks", which in silicon dioxide comprise of an underdense core surrounded by an overdense shell [11]. If the ion track and the NP dimensions are comparable, elongation can be achieved from single events [12] and appears to be related to the ion track dimensions [13,14]. When the ion passes through the MNP, it increases its temperature starting from the metal-dielectric boundary inwards, as the thermal conductivity of silicon dioxide is two orders of magnitude lower than that of most metals and therefore, acts as a thermal insulator [15], resulting in complete NP melting. As the ion track formation time-scale is comparable to that of NP melting, the NP expands via longitudinal flow into the underdense core of the ion track and subsequent recrystallization [16].

In this work we present experimental results of the shape transformation of Au and Ag NPs located at the interface of amorphous silicon nitride and silicon dioxide thin films upon irradiation with 185 MeV Au ions. We selected silicon nitride due to the existing applications and the higher refractive index compared to silicon dioxide. Under these conditions, a shape transformation process with different modification rates is expected, as silicon nitride possesses a smaller track radius and higher thermal conductivity (still one order of magnitude below the value for metals) in comparison with amorphous silicon dioxide. We discuss our experimental results with respect to the thermal spike calculations of the time evolution of ion track formation in both materials.

2. Material and methods

An amorphous silicon nitride layer with a thickness of 600 nm was first deposited on top of a c-Si(100) wafer by plasma-enhanced chemical vapor deposition (PECVD). Afterwards, Au or Ag layers (5 nm in thickness) were deposited on top by thermal

* Corresponding author.
E-mail address: pablo.mota@anu.edu.au (P. Mota-Santiago).

http://dx.doi.org/10.1016/j.nimb.2017.03.068
0168-583X/

Please cite this article in press as: P. Mota-Santiago et al., Elongation of metallic nanoparticles at the interface of silicon dioxide and silicon nitride, Nucl. Instr. Meth. B (2017), http://dx.doi.org/10.1016/j.nimb.2017.03.068

evaporation. Finally, a 500 nm thick top layer of amorphous silicon dioxide was deposited by PECVD. Subsequently, to promote the formation of nearly spherical Au and Ag NPs, rapid thermal annealing (RTA) was carried out at 1000 °C and 800 °C, respectively, in N_2 atmosphere for 120 s.

Swift heavy-ion irradiation of the samples was performed with 185 MeV Au^{13+} ions at the 14UD ion accelerator at the Australian National University in normal incidence with two fluences (0.3 and 1×10^{14} cm^{-2}) at room temperature. The corresponding electronic stopping powers were calculated with the SRIM2013 code [17] to 49.7, 41.5, 23.3 and 16.1 keV/nm for Au, Ag, silicon nitride and silicon dioxide, respectively. The samples were characterized by cross-section transmission electron microscopy (X-TEM) and by high angular annular dark field (HAADF) with a JEOL 2100F microscope operated at 200 kV. The former allows the characterization of size and shape while the latter, due to the high contrast, permits the identification of small features such as MNPs with radius equal or less than 2 nm. Preparation of samples for TEM

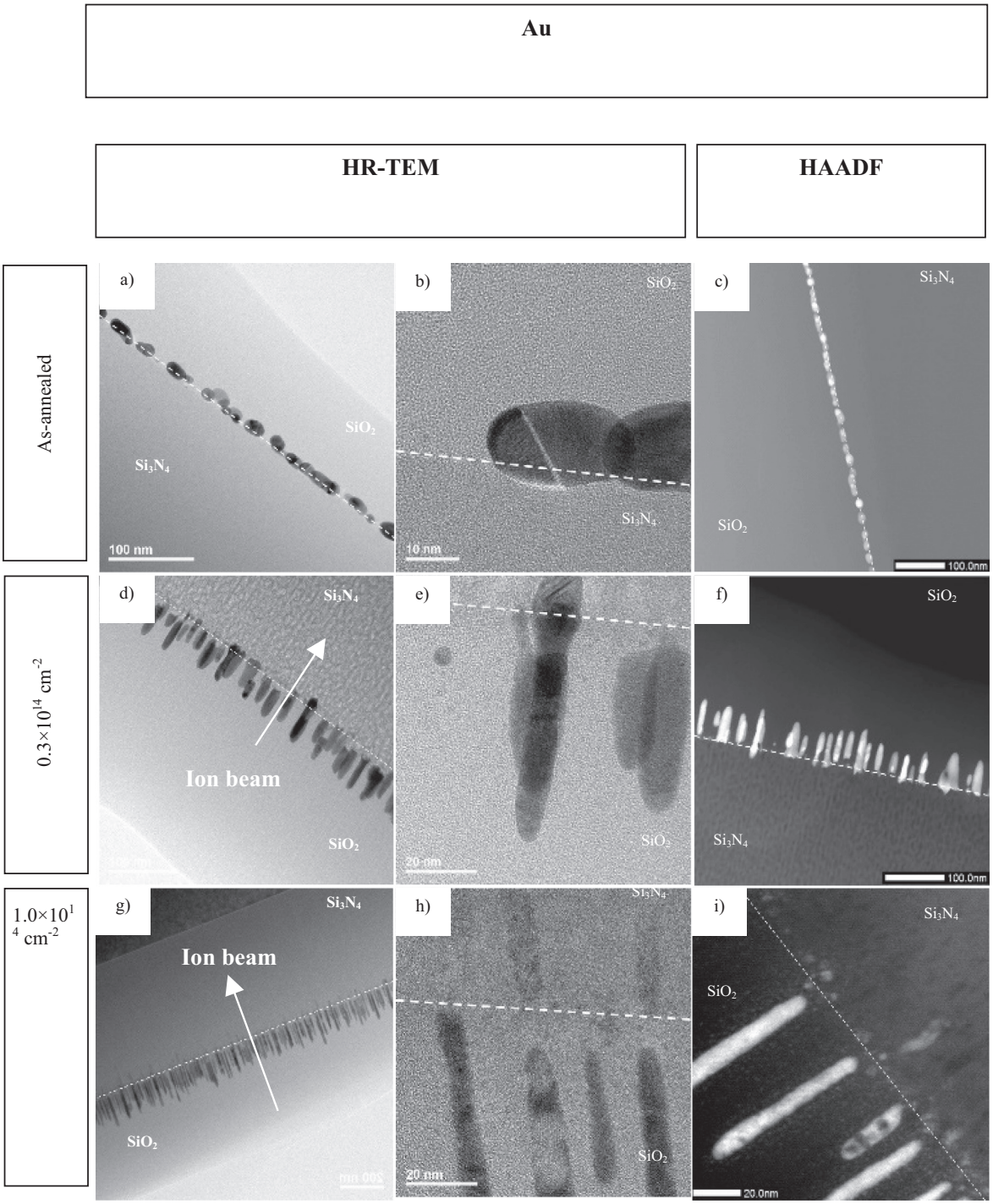

Fig. 1. Cross-section HR-TEM (a), (b), (d), (e), (g) and (h)) and HAADF in STEM mode (c), (f) and (i)) pictures of Au NPs. Images (a), (d) and (g) were taken at low magnification to observe the location of the NPs in the sample before and after being irradiated. (b), (e) and (h) are images at high magnification at the interface. HAADF pictures (c), (f) and (i)) near the interface showing structural changes induced by the irradiation fluence and the occurrence of very small NPs. White dashed lines were added to emphasize the interface location.

Please cite this article in press as: P. Mota-Santiago et al., Elongation of metallic nanoparticles at the interface of silicon dioxide and silicon nitride, Nucl. Instr. Meth. B (2017), http://dx.doi.org/10.1016/j.nimb.2017.03.068

after mechanically dimpling to a final thickness of 10 μm was performed with a precision ion polishing system (PIPS) GATAN model 961 at −165 °C to minimize unwanted warming up of the sample.

The temperature time evolution in the dielectric layers around the ion paths was estimated using the inelastic Thermal Spike (i-TS) model [18]. The free electron gas approximation suggested by

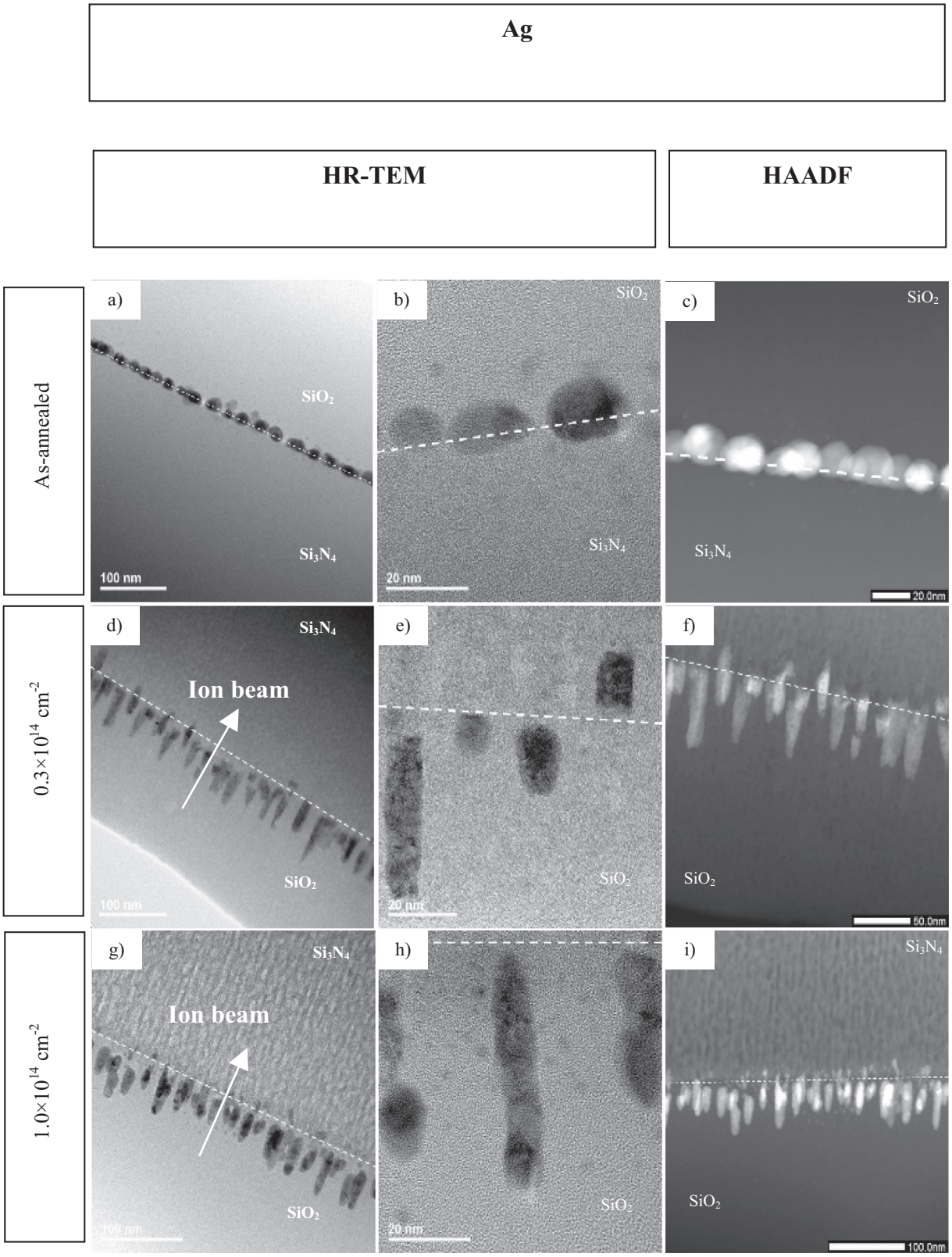

Fig. 2. Cross-section HR-TEM (a), (b), (d), (e), (g) and (h)) and HAADF in STEM mode (c), (f) and (i)) pictures of Ag NPs. Images (a), (d) and (g) were taken at low magnification to observe the location of the NPs in the sample before and after being irradiated. (b), (e) and (h) are images at high magnification at the interface. HAADF pictures (c), (f) and (i)) at the interface showing structural changes induced by the irradiation fluence and the occurrence of very small NPs. White dash lines were added to emphasize the interface location.

Please cite this article in press as: P. Mota-Santiago et al., Elongation of metallic nanoparticles at the interface of silicon dioxide and silicon nitride, Nucl. Instr. Meth. B (2017), http://dx.doi.org/10.1016/j.nimb.2017.03.068

Dufour et al. [15] was followed to determine the parameters of the electronic subsystem while for the physical parameters of both layers we considered the values used in [15] and [19]. The value of the electron-phonon coupling (λ) of each material was calculated considering the experimental optical band gap [20] and their empirical relationship with λ [21]. While more comprehensive numerical modeling would be desirable, as in the case of Au NPs embedded in amorphous silicon dioxide [15], for the purposes of this study the differences in the temperature evolution for both materials following from our numerical calculations provide first insights for explaining the experimental results observed.

3. Results and discussion

Figs. 1and 2 show the shape transformation of nearly spherical MNPs when located at the interface of the two dielectric materials after irradiation with two different ion fluences. At the selected fluences of 0.3×10^{14} cm^{-2} and 1×10^{14} cm^{-2} well-aligned and elongated single layer NPs can be observed (Figs. 1(d), (g) and 2(d), (g)).

Thermal deposition of 5 nm layers followed by an RTA process leads to the formation of single layers of nearly spherical NPs with an average diameter of 16.0 ± 4.5 nm in the case of Au, and 18.1 ± 5.5 nm for Ag (Figs. 1(a)–(c) and 2(a)–(c)). The advantages of this procedure is the reduction in NP size dispersion while ensuring contact with both layers (Figs. 1 (b) and 2 (b)), as well as avoiding additional structural damage as in the case of ion implantation [18]. For Ag NPs (Fig. 2(b)), we observe small clusters formed around the interface with a mean diameter of 2 nm, probably generated during the deposition of the top silicon dioxide layer at 600 °C.

In the case of Au NPs, after irradiation with 0.3×10^{14} cm^{-2} Au ions we observe a shape transformation starting from the interface and mainly into the silicon dioxide layer, yet we observe few cases of elongation into the silicon nitride ((Fig. 1(e) and (f)). After irradiation, the MNPs progress quickly into nano-rods with higher aspect ratios than previous results in thermally grown silicon dioxide, yet a slightly decrease in the mean width at higher fluences probably leading to a smaller saturation width than the previously reported, approximately 10 nm [11,22,23]. The decrease in the value of the saturation width confirms the critical role played by the matrix in the shape transformation process [23]. From previous results on thermally grown silicon dioxide, the ion track dimensions impose an upper boundary on the saturation widths on Au NPs [22,23]. In the current case, the silicon dioxide layer was grown by PECVD with some H content, revealing a different local structure and density compared to thermal oxide. This can influence the thermal properties of the matrix and may result in the observed decrease in the saturation width, yet is in agreement with the previous studies [22,23]. The observed nano-rods exhibit a high aspect ratio with a width of 11.2 ± 5.2 nm and a length of 42.2 ± 18.1 nm when irradiated with 0.3×10^{14} cm^{-2}. At the highest fluence (1×10^{14} cm^{-2}), the majority of the formed nano-rods (8.6 ± 2.1 nm in width and 77.1 ± 24.8 nm in length) appear to be no longer in contact with the interface (Fig. 1(i)) forming a gap of 2–4 nm populated by clusters of 2 ± 0.8 nm in radius (Fig. 1(h) and (i)).

Elongation is also achieved in the case of Ag NPs at both irradiation fluences. For the first case (0.3×10^{14} cm^{-2}), elongated NPs with a width of 13.9 ± 5.2 nm and a length of 18.2 ± 6.3 nm in the ion beam direction were observed, also preferentially into silicon dioxide where cylindrical and conical geometries were observed (Fig. 2(d) and (f)), yet more cases of elongation into both layers were observed than for Au NPs. Similar to the case of Au NPs, when the fluence is increased to 1×10^{14} cm^{-2} an increment in the density of NPs distanced from the interface was observed (Fig. 2 (g)–(i)). The corresponding dimensions of the observed nano-rods were 12.3 ± 4.1 nm in width and 25.1 ± 8.9 nm in length, demonstrating a lower elongation rate for Ag compared to Au. Fig. 2(h) shows very small clusters around the interface and surrounding the nano-rods, due to the pre-existent small NPs it is not possible to distinguish if their origin is due to ion irradiation effects of the NPs or due to the initial NP formation.

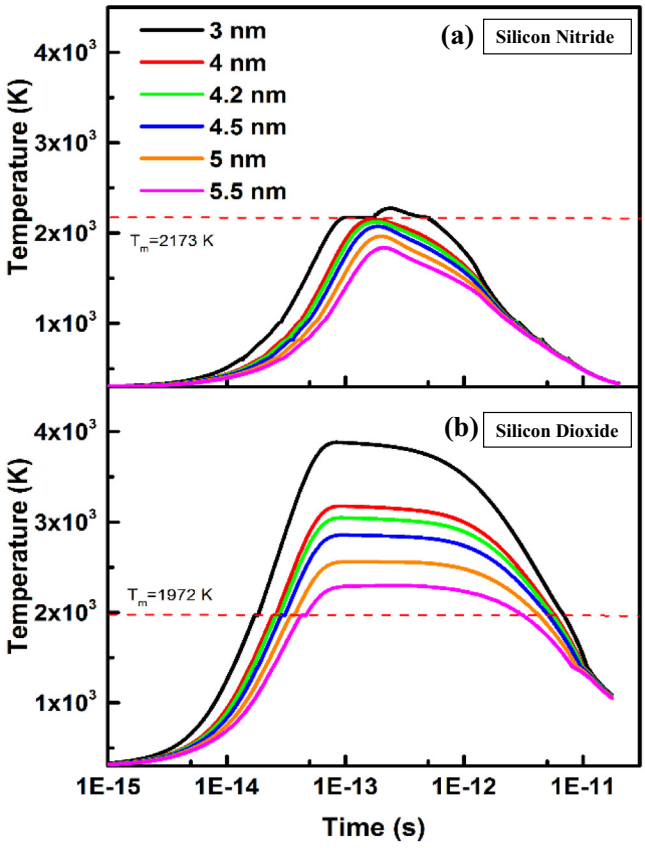

Fig. 3. Time evolution of lattice temperature calculated by the i-TS model at different radial distances from the ion path: 3, 4, 4.2, 4.5, 5, 5.5 nm for (a) silicon nitride and (b) silicon dioxide. Red dashed lines were added to highlighted the typical transition temperature considered above which an ion track is formed for each dielectric. (For interpretation of the references to color in this figure legend, the reader is referred to the web version of this article.)

As the MNPs are in contact with both materials, after the passage of the energetic Au ion an ion track is formed in each layer, influencing the shape elongation process. Independently, we have characterized the ion track formation in silicon nitride and silicon dioxide layers by small angle X-ray scattering (SAXS), which under similar irradiation energies exhibit an ion track radius of 4.2 ± 0.1 nm for silicon nitride and 5.5 ± 0.1 nm for silicon dioxide formed by underdense core surrounded by an overdense shell, where the dimensions for the core are similar for both materials. A detailed analysis is available in [11,20,24]. As described by Leino et al. [16], for the case of Au NPs in silicon dioxide, between 5 and 20 ps after the ion passage, the NP elongation process occurs via metal flow into the underdense region. Subsequently, the temperature decreases below the glass transition of silicon dioxide terminating the transformation step. Silicon nitride possess a thermal conductivity much higher than silicon dioxide, and thus the track formation process can occur in a fraction of the time it takes in silicon dioxide, limiting the time for the flow of metal.

The lattice temperature evolution with time at different distances from the ion path (3, 4, 4.2, 4.5, 5 and 5.5 nm) was calculated and is plotted in Fig. 3. We are interested in the regions

Please cite this article in press as: P. Mota-Santiago et al., Elongation of metallic nanoparticles at the interface of silicon dioxide and silicon nitride, Nucl. Instr. Meth. B (2017), http://dx.doi.org/10.1016/j.nimb.2017.03.068

around 4 nm and 5.5 nm as they correspond to the track radius in silicon nitride (4.2 ± 0.1 nm) and silicon dioxide (5.5 ± 0.1 nm) [20,24]. From Fig. 3, we estimated ion tracks radii to approximately 4.1 ± 0.4 nm and 5.8 ± 0.3 nm, in agreement with the experimental values. The optical band gap was measured by spectral reflectometry to be 4.9 ± 0.3 eV for silicon nitride and 9.1 ± 0.2 eV for silicon dioxide. As a consequence of the difference in the optical band gap, the corresponding electron-phonon coupling is relatively low in silicon nitride $g_{Si3N4} = 0.52 \times 10^{13}$ W/cm^3 K^{-1} in comparison with the case of silicon dioxide ($g_{SiO2} = 1.25 \times 10^{13}$ W/cm^3 K^{-1}) leading to a lower energy transfer from the electronic subsystem into the lattice, and a smaller ion track radius. In addition, as apparent from Fig. 3 the higher thermal conductivity 11.0×10^{-2} W/cm K^{-1} of silicon nitride compared to silicon dioxide 3.0×10^{-2} W/cm K^{-1} leads to an increased energy dissipation, therefore reducing the time period for ion track formation also limiting the interaction of the melted NP with the ion track. We believe that this is at least in part the reason for the predominant elongation into silicon dioxide.

4. Conclusions

In this work we presented experimental observations regarding the shape transformation of nearly spherical NPs with average diameters 16–18 nm after irradiation with 185 MeV Au ions at the interface of silicon nitride and silicon dioxide layers. The resulting elongation process occurs preferentially towards the silicon dioxide layer while creating a high density of very small nanostructures with an average radius of 2 nm at the interface. Thermal Spike calculations suggest that the different timescales of ion track formation in both dielectrics plays an important role and favors the elongation process in silicon dioxide.

Acknowledgements

P. Mota-Santiago would like to thank the Consejo Nacional de Ciencia y Tencologia (CONACyT) for financial support. The authors acknowledge the facilities, and the scientific and technical assistance, of the Australian Microscopy & Microanalysis Research Facility at the Centre of Advanced Microscopy, the Australian National University. We acknowledge access to NCRIS facilities (ANFF and the Heavy Ion Accelerator Capability) at the Australian National University. P. Kluth and M. C. Ridgway thank the Australian Research Council for financial support.

References

[1] C. D'Orléans, J.P. Stoquert, C. Estournès, C. Cerruti, J.J. Grob, J.L. Guille, F. Haas, D. Muller, M. Richard-Plouet, Phys. Rev. B 67 (2003) 220101.
[2] H. Amekura, N. Ishikawa, N. Okubo, M.C. Ridgway, R. Giulian, K. Mitsuishi, Y. Nakayama, C. Buchal, S. Mantl, N. Kishimoto, Phys. Rev. B 83 (2011) 205401.
[3] M. Bayle, C. Bonafos, P. Benzo, G. Benassayag, B. Pécassou, L. Khomenkova, F. Gourbilleau, R. Carles, Appl. Phys. Lett. 107 (2015) 101907.
[4] J.A. Reyes-Esqueda, C. Torres-Torres, J.C. Cheang-Wong, A. Crespo-Sosa, L. Rodriguez-Fernandez, C. Noguez, A. Oliver, Large optical birefringence by anisotropic silver nanocomposites, Opt. Express 16 (2008) 710–717.
[5] P.E. Mota-Santiago, A. Crespo-Sosa, J.L. Jiménez-Hernández, H.G. Silva-Pereyra, J.A. Reyes-Esqueda, A. Oliver, Appl. Surf. Sci. 259 (2012) 574–581.
[6] O. Sánchez-Dena, P. Mota-Santiago, L. Tamayo-Rivera, E.V. García-Ramírez, A. Crespo-Sosa, J.A. Reyes-Esqueda, Opt. Mater. Express 4 (2014) 92–100.
[7] S. Klaumunzer, Nucl. Instrum. Methods Phys. Res. B 244 (2006) 1–7.
[8] A. Oliver, J.A. Reyes-Esqueda, J.C. Cheang-Wong, C.E. Román-Velázquez, A. Crespo-Sosa, L. Rodríguez-Fernández, J.A. Seman, C. Noguez, Phys. Rev. B 74 (2006) 245425.
[9] E.A. Dawi, G. Rizza, M.P. Mink, A.M. Vredenberg, F.P. Habraken, J. Appl. Phys. 105 (2009) 074305.
[10] C. Noguez, J. Phys. Chem. C 111 (2007) 3806–3819.
[11] P. Kluth, C.S. Schnohr, O.H. Pakarinen, F. Djurabekova, D.J. Sprouster, R. Giulian, M.C. Ridgway, A.P. Byrne, C. Trautmann, D.J. Cookson, K. Nordlund, M. Toulemonde, Phys. Rev. Lett. 101 (2008) 175503.
[12] M.C. Ridgway, P. Kluth, R. Giulian, D.J. Sprouster, L.L. Araujo, C.S. Schnohr, D. Llewellyn, A.P. Byrne, G.J. Foran, D.J. Cookson, Nucl. Instrum. Methods Phys. Res. B 267 (2009) 931–935.
[13] R. Giulian, F. Kremer, L.L. Araujo, D.J. Sprouster, P. Kluth, P. Fichtner, A.P. Byrne, M.C. Ridgway, Phys. Rev. B 82 (2010) 113410.
[14] M.C. Ridgway, R. Giulian, R. Sprouster, P. Kluth, L.L. Araujo, D.J. Llewellyn, A.P. Byrne, F. Kremer, P. Fichtner, G. Rizza, H. Amekura, M. Toulemonde, Phys. Rev. Lett. 106 (2011) 095505.
[15] C. Dufour, V. Khomenkov, G. Rizza, M. Toulemonde, J. Phys. D: Appl. Phys. 45 (2012) 065302.
[16] A.A. Leino, O.H. Pakarinen, F. Djurabekova, K. Nordlund, P. Kluth, M.C. Ridgway, Mater. Res. Lett. 2 (2013) 37–42.
[17] J.F. Ziegler, J.P. Biersack, U.L. Littmark, The Stopping and Range of Ions in Matter, Pergamon, New York, 1985.
[18] W. Wesch, E. Wendler, Ion Beam Modification of Solids, Springer International Publishing, 2016.
[19] T. Kitayama, Y. Morita, K. Nakajima, K. Narumi, Y. Saitoh, M. Matsuda, M. Sataka, M. Tsujimoto, S. Isoda, M. Toulemonde, K. Kimura, Nucl. Instrum. Methods Phys. Res. B 356–357 (2015) 22–27.
[20] P. Mota-Santiago, T. Bierschenk, F. Kremer, A. Nadzri, H. Vazquez, F. Djurabekova, K. Nordlund, C. Trautmann, S. Mudie, M.C. Ridgway, P. Kluth, in preparation.
[21] M. Toulemonde, C. Dufour, A. Meftah, E. Paumier, Nucl. Instrum. Methods Phys. Res. B 166–167 (2000) 903–912.
[22] P. Kluth, R. Giulian, D.J. Sprouster, C.S. Schnohr, A.P. Byrne, D.J. Cookson, M.C. Ridgway, Appl. Phys. Lett. 94 (2009) 113107.
[23] M.C. Ridgway, R. Giulian, D.J. Sprouster, P. Kluth, L.L. Araujo, D.J. Llewellyn, A.P. Byrne, Phys. Rev. Lett. 106 (2011) 095505.
[24] P. Mota-Santiago, D. Schauries, A. Nadzri, K. Vora, M.C. Ridgway, P. Kluth, EPJ Web Conf. 91 (2015) 00008.

Please cite this article in press as: P. Mota-Santiago et al., Elongation of metallic nanoparticles at the interface of silicon dioxide and silicon nitride, Nucl. Instr. Meth. B (2017), http://dx.doi.org/10.1016/j.nimb.2017.03.068